

EFFECTS OF LOADING RATE AND SPECIMEN CONFIGURATION ON THE DUCTILE-BRITTLE TRANSITION IN POLY(PROPYLENE)

Z. Major² and R.W. Lang^{1,2}

¹ Institute of Materials Science and Testing of Plastics,
University of Leoben

² Institute of Polymer Technology,
Joanneum Research Forschungsges.m.b.H.
A-8700 Leoben, Austria

ABSTRACT

To gain more insight into the fracture behavior of poly(propylene) (PP), specifically on the loading rate dependent ductile-brittle transition a fracture mechanics methodology was developed and applied. For this purpose, loading rate and geometry effects (various relative crack length values, SENB vs. C(T) specimens, and plain-sided vs. side-grooved specimens) on the fracture behavior of three PP types were investigated by performing fracture toughness tests over 6 decades of loading rates. Using different definitions of J-integral for data reduction, which properly account for the temperature rate and geometry dependence of the fracture behavior of plastics, a procedure is proposed to better characterize the ductile-brittle transition in the semi-brittle crack extension region and in terms of an “embrittlement point” at high loading rates. Comparing the various PP types investigated, differences in the ductile-brittle transition behavior on the loading rate scale of up to 4 orders of magnitude were determined. Moreover, it was found that for SENB specimens the “embrittlement point” depends on the relative crack length, a/W .

INTRODUCTION

For many applications of engineering plastics, fracture behavior under monotonic and impact loading conditions is of prime practical importance. In this context it is well known that fracture properties of plastics are significantly affected by the loading rate, the temperature and the local (if notches or cracks are present) and global stress state. As a result of the complex effects of these parameters, fracture values determined by conventional test methods are only of very limited use for material characterization and engineering design purposes, especially at high loading rates (e.g., unnotched and notched Charpy fracture energies).

The limitations associated with conventional test methods may at least in principle be overcome by the use of appropriate fracture mechanical approaches, which properly account for the temperature and rate dependence of the mechanical behavior of plastics. In general, a brittle-to-ductile transition in the fracture behavior occurs, as the test temperature is increased from low to high temperatures. Due to the viscoelastic nature of plastics, this brittle-to-ductile transition depends on the loading rate and also on the local and global stress state. It is the objective of this paper, to present and discuss results of systematic experimental investigations on the rate and specimen configurations dependence of fracture properties in three grades of poly(propylene) (PP). Based on the experimental results various data reduction schemes are proposed to define the ductile-brittle transition on the loading rate scale.

EXPERIMENTAL

Materials

Various grades of PP (un-nucleated random-copolymer PP (u-PP(RC))-1, α -nucleated homopolymer PP (α -PP(H)) and β -nucleated homopolymer PP (β^+ -PP(H)) were used for this study. The materials were supplied as compression molded sheets.

Specimen configuration and preparation

Side-grooved single edge notched bending specimens (SENB-SG) with relative crack length values, a/W , ranging from 0.1 to 0.7 and plain-sided compact type specimens (C(T)-PS) as well as side-grooved compact type specimens (C(T)-SG) with relative crack length values of 0.5 were included in the investigation.

The nominal thickness of the specimens was 15 mm, and the nominal depth of the side grooves was 1.5 mm on each specimen side. The V-notch of the specimens and the side grooves were machined using special cutting tools (V-notch angle and side groove angle of 45 °). A razor blade was pressed into the V-notch tip for approximately 2 mm prior to testing to generate a sharp precrack.

Test procedure and data reduction

All tests were performed with a high rate servohydraulic test system (Polymer Test System MTS 831.59, MTS Systems Corp., MN, USA), which was instrumented according to the requirements of the various low and high rate fracture tests. The test temperature was 23 °C and the loading rates were varied from 0.01 to 8000 mm/s. Further details as to the test equipment are described in [1].

Two types of test series were performed. In the first case, SENB-SG, C(T)-PS and C(T)-SG specimens were tested as single specimens fractured at various loading rates yielding corresponding fracture parameters for these loading rates. As the methodology of linear elastic fracture mechanics (LEFM) to determine the fracture toughness is not applicable for the high degree of non-linearity observed, a data reduction scheme based on various values of the J-integral was applied and corresponding values for J were determined as follows:

$$J = \frac{\eta(a/W)U}{B(W-a)} \quad (1)$$

where U is the fracture energy up to the relevant force (F_m for J_m or J_c and F_u for J_u), $\eta(a/W)$ is a crack length dependent geometry factor, B is the specimen thickness (corresponding to B_{SG} , the net thickness without side-grooves for side-grooved specimens), W is the specimen width and a is the crack length. While J_c is applicable to characterize quasi-brittle failure behaviour (quasi-linear load-displacement behavior with a sharp load drop at the point of fracture), J_m and J_u refer to J-integral definitions in which the peak loads, F_m , and the ultimate loads, F_u , respectively, are used in the data reduction procedure for materials with non-linear displacement traces and a certain amount of stable crack extension prior to ultimate specimen failure. Details for the determination of the geometry factor, $\eta(a/W)$, are given in [4,5]. All fracture energy values were corrected by the indentation energy according to a procedure described in [3].

In the second case, load-displacement curves were recorded for various testing rates using several specimens to generate rate specific crack extension curves (R-curves). These tests were performed according to proposals by ASTM [2] and ESIS [3]. In this case, $J_{0.2}$ values were determined, which characterize the fracture resistance at 0.2 mm of crack extension. For higher testing rates (over 1 to 10 mm/s depending on the material), a special experimental procedure was developed to determine R-curves. In these tests the actuator movement was stopped at various predefined deformations prior to total specimen fracture and the load and displacement data were recorded. The crack extension dependent J-integral values were determined according to data reduction procedures described elsewhere [4].

RESULTS AND DISCUSSION

Load-displacement traces for α -PP(H) and for β^+ -PP(H) are shown for the SENB-SG specimen configuration in Figs. 1 and 2, respectively, for various loading rates and two different a/W values. While α -PP(H) reveals quasi-brittle fracture behavior at all loading rates and for both a/W values (Fig. 1), β^+ -PP(H) clearly exhibits more ductile fracture behavior in the investigated loading rate range (Fig. 2). However, of major importance with regard to specimen configuration effects, in the loading rate range from 1 to 1000 mm/s the load-displacement curves for β^+ -PP(H) with $a/W=0.1$ reveal quasi-brittle fracture or at least semi-brittle crack instability (Fig. 2a), while ductile crack extension was observed over the same loading rate range for specimens with $a/W=0.66$ (Fig. 2b). In other words, the ductile-brittle transition with increasing testing rate occurs at significantly lower testing rates for smaller a/W values.

Analogously, load-displacement traces for plain-sided and side-grooved C(T) specimens of u-PP(RC)-1 and β^+ -PP(H) are shown in Figs. 3 and 4 for various loading rates. As expected, comparing the behavior of C(T)-PS and C(T)-SG specimens illustrates that for both materials the rate dependent ductile–brittle transition occurs at lower testing rates for side-grooved specimens. Although, this effect is apparently more pronounced for u-PP(RC)-1 (Fig. 3), a significant difference between plain-sided and side-grooved specimens may also be noted for β^+ -PP(H) at higher loading rates (Fig. 4). That is the occurrence of crack arrest in plain-sided specimens at testing rates between 250 and 1000 mm/s, a phenomenon which was never observed for side-grooved specimens of this material type. Peculiarly, for u-PP(RC)-1 the opposite behavior was observed. That is crack arrest was found to occur in side-grooved specimens (although over a very limited loading rate range of around 100 mm/s) and not in plain-sided specimens (Fig. 3).

To summarize these findings, a rate dependent ductile-brittle transition was found to occur. At low loading rates, specimens fail via a stable crack growth process up to ultimate specimen fracture (ductile failure). With increasing loading rate, specimen failure occurs by an initial stable crack growth process followed by unstable crack extension (semi-brittle failure). The contribution of the initial stable crack growth process is reduced with increasing loading rate and finally suppressed at high loading rates (quasi-brittle failure without significant stable crack growth).

As to the convenient engineering use of the results of such fracture tests an important question arises. That is, which fracture mechanical parameter(s) and/or parameters functions can characterize this complex transition behavior (i.e., stress based or energy based parameters, single parameter, several parameters or parameter functions). In principle, different J-integral approaches and values may be defined to describe the various fracture processes.

Rate dependent R-curves may be used to characterize both, the crack initiation process and the stable crack growth behavior. R-curves of this type illustrating the behavior of u-PP(RC)-1 and β^+ -PP(H) for two specimen configurations (plain-sided and side-grooved) and various loading rates are shown in Figs. 5 and 6, respectively. As a result of the higher constraint in the crack tip region, for a given loading rate (in this case 1 mm/s) the presence of side grooves results in a significant shift of the R-curves towards smaller J values for both materials. In terms of materials specific fracture behavior and as conservative crack extension characterization this implies that, R-curves from side-grooved specimens are to be preferred.

With regard to the effect of loading rate, different results were obtained for side-grooved C(T)-specimens of u-PP(RC)-1 and β^+ -PP(H). While the R-curves for the former material in the loading rate range from 0.1 to 100 mm/s do not reveal any significant differences (Fig. 5), the J- Δa -curves are continuously shifted towards smaller J values with increasing testing rate (Fig. 6). A similar effect of the testing rate is shown in Fig. 7 for side-grooved SENB specimens of β^+ -PP(H). For this test series, specimens with two values of a/W (0.2 and

0.5) were investigated. The results in Fig. 7 indicate that the R-curves while being strongly loading rate dependent do not reveal any significant geometry dependence.

To establish a well-defined engineering criterion for the ductile-brittle transition on the loading rate scale taking into account the geometry effects, an engineering procedure was developed and applied [6]. First the load-displacement curves were analyzed to achieve data for J-integral definitions in terms of J_c , J_m and J_u , respectively, as described above. The various results of this data reduction procedure are shown in Figs. 8 and 9 for both material types investigated and for side-grooved specimens with a/W values ranging from 0.12 to 0.66 as a function of loading rate (in terms of dJ/dt). While clearly separated curves are obtained especially for J_m and J_u at low loading rates, all curves are seen to converge at high loading rates. The point of convergence indicates the transition to quasi-brittle behavior and may be defined as “embrittlement point” on the loading rate scale. Of particular importance is the observation that the location of the “embrittlement point” also depends on the relative crack length, a/W .

Hence, in Fig. 10 these “embrittlement points” (i.e., dJ/dt_{emb}) are depicted as a function of a/W for both materials investigated. Clearly, β^+ -PP(H) may sustain loading rates which are 3 to 4 orders of magnitude higher than those for α -PP(H), before quasi-brittle failure takes place. Also worth mentioning when comparing these two materials is that α -PP(H) exhibits a stronger a/W dependence.

Finally, in terms of the ductile-brittle transition range also of importance are the degree of increase of the J_m and J_u values with decreasing loading rates on the one hand and the differences between J_u and J_m in this range on the other hand. Here too β^+ -PP(H) proves to be superior over α -PP(H) (compare Figs. 8 and 9).

CONCLUSIONS

In this study loading rate and geometry effects (various relative crack length values, SENB vs. C(T) specimens, and plain-sided vs. side-grooved specimens) on the ductile-brittle transition of three PP types were investigated by performing fracture toughness tests over 6 decades of loading rates. While from a material science point of view R-curves offer significant insight as to various crack extension mechanisms (crack growth initiation and propagation), it is difficult to establish a well-defined criterion for the ductile-brittle transition on the loading rate scale based on such curves. Hence a procedure was applied to better characterize the ductile-brittle transition in the semi-brittle crack extension region and in terms of an “embrittlement point” at high loading rates. It could be shown that at least for SENB specimens the “embrittlement point” on the loading rate scale depends on the relative crack length, a/W . Furthermore, the PP types investigated were found to reveal significant differences with regard to their ductile-brittle transition behavior.

REFERENCES:

1. Z. Major, R.W.Lang: Mech. of Time Dep. Mat. 11-13.1995, Ljubljana, p. 304-309
2. ASTM E 1737-96: Standard Test Method for J-Integral Characterization of Fracture Toughness, Annual Book of ASTM Standards, Vol 03.01., Philadelphia
3. ESIS TC4: Testing Protocol for J-Crack Growth R-Curve Test on Plastics, 1995
4. J.A. Joyce: ASTM Manual on Elastic.Plastic Fracture Laboratory Test Procedure, ASTM MNL 27, 1996
5. K.H. Schwalbe et al.: EFAM ETM 97, GKSS 98/E/6, Geesthacht, 1998
6. Z. Major, R.W.Lang: Deformation Yield and Fracture of Polymers Conference, 12-15.2000, Cambridge (submitted)

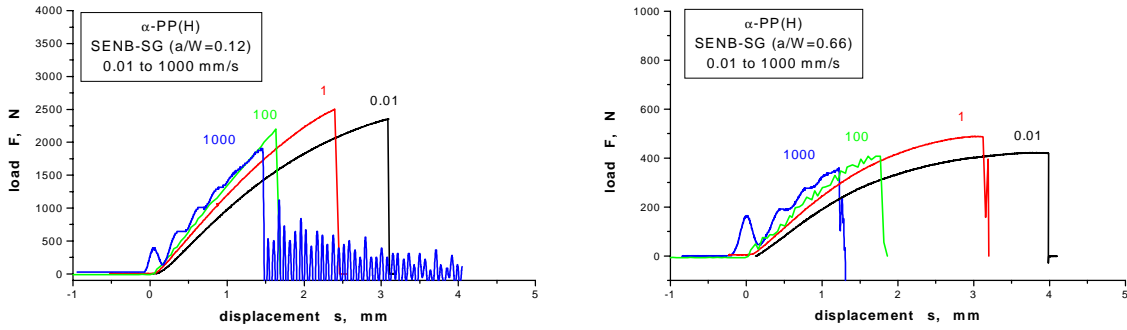


Fig. 1: Load-displacement curves for SENB-SG specimens of α -PP(H) at various testing rates

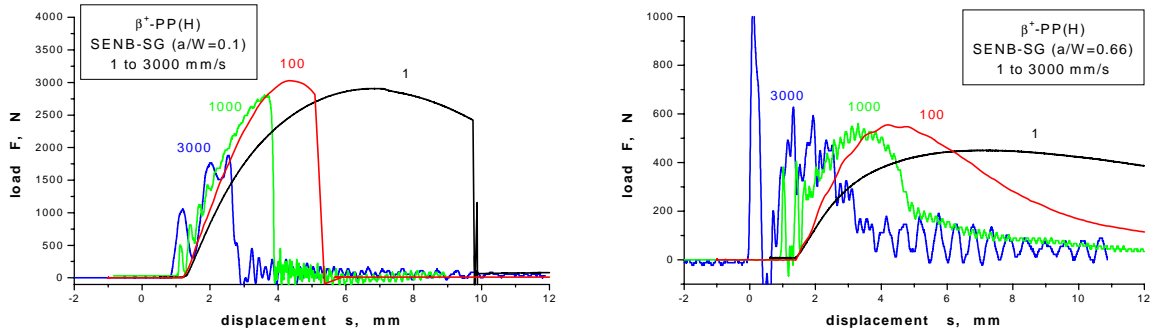


Fig. 2: Load-displacement curves for SENB-SG specimens of β^+ -PP(H) at various testing rates

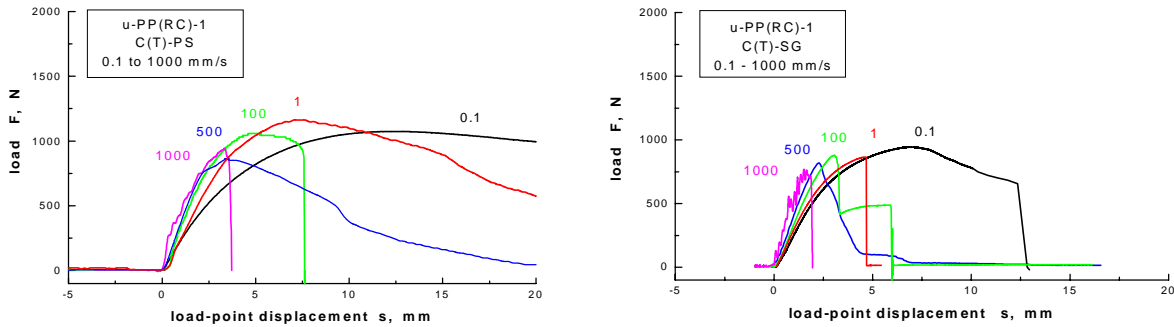


Fig. 3: Load-displacement curves for C(T)-PS and C(T)-SG specimens of u-PP(RC)-1 at various testing rates

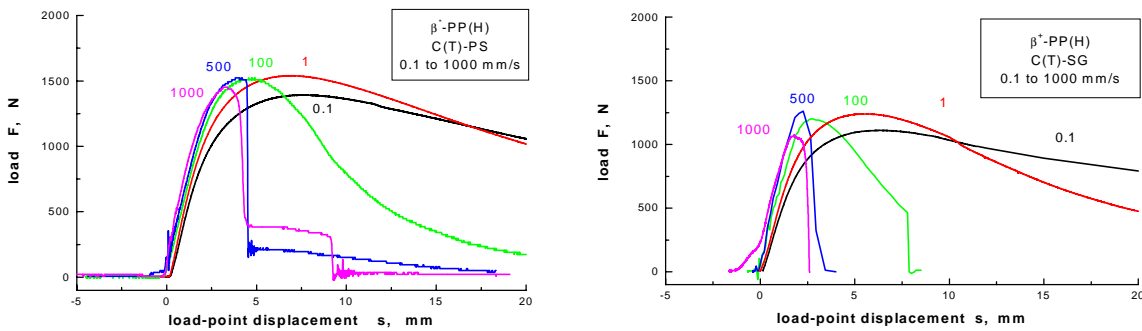


Fig. 4: Load-displacement curves for C(T)-PS and C(T)-SG specimens of β^+ -PP(H)-1 at various testing rates

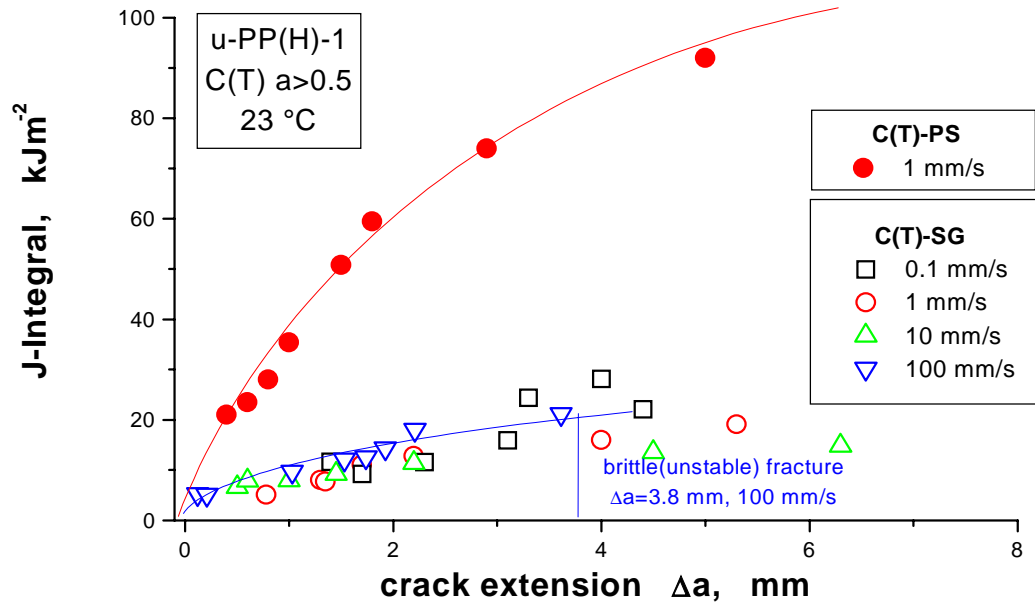


Fig. 5: J- Δa -curves for plain-sided (C(T)-PS) and side-grooved (C(T)-SG) specimens of u-PP(RC)-1 at various testing rates

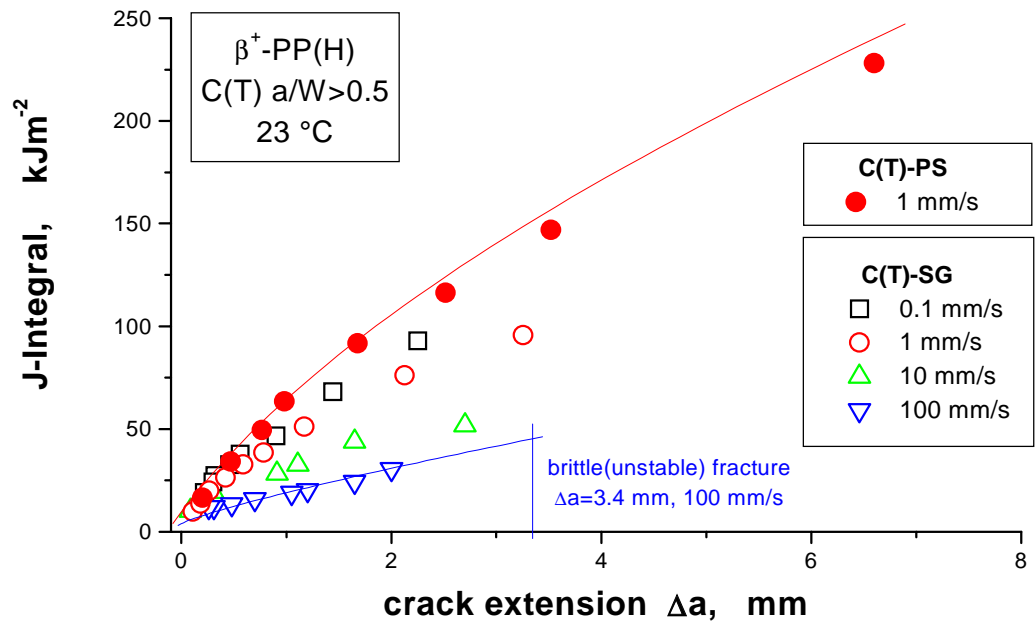


Fig. 6: J- Δa -curves for plain-sided (C(T)-PS) and side-grooved (C(T)-SG) specimens of β^+ -PP(H) at various testing rates

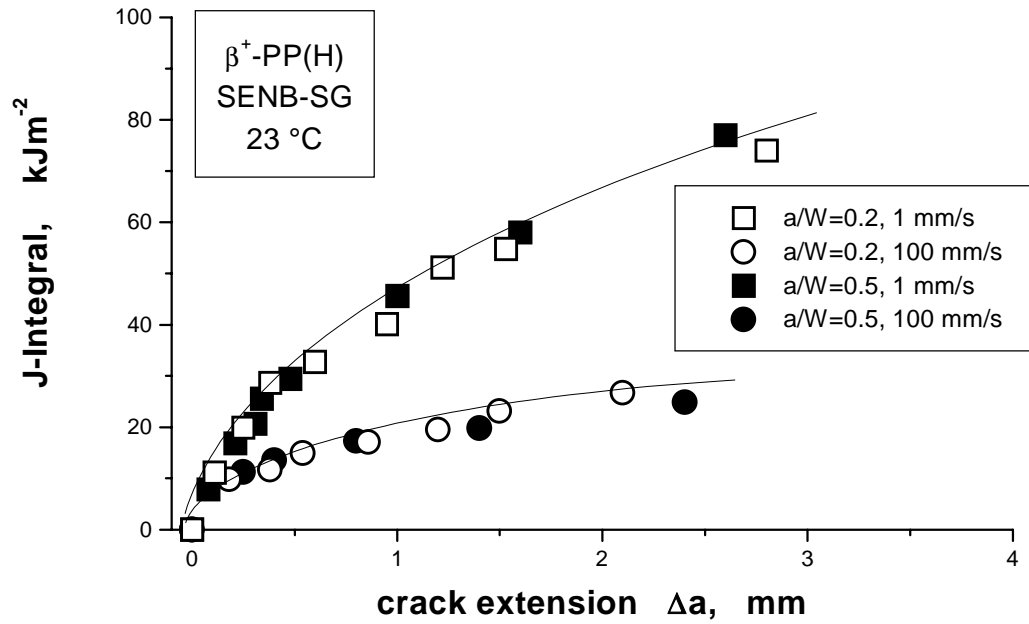


Fig. 7: J- Δa -curves for SENB-SG specimens of β^+ -PP(H) with relative crack length values of 0.2 and 0.5 at testing rates 1 mm/s and 100 mm/s, respectively

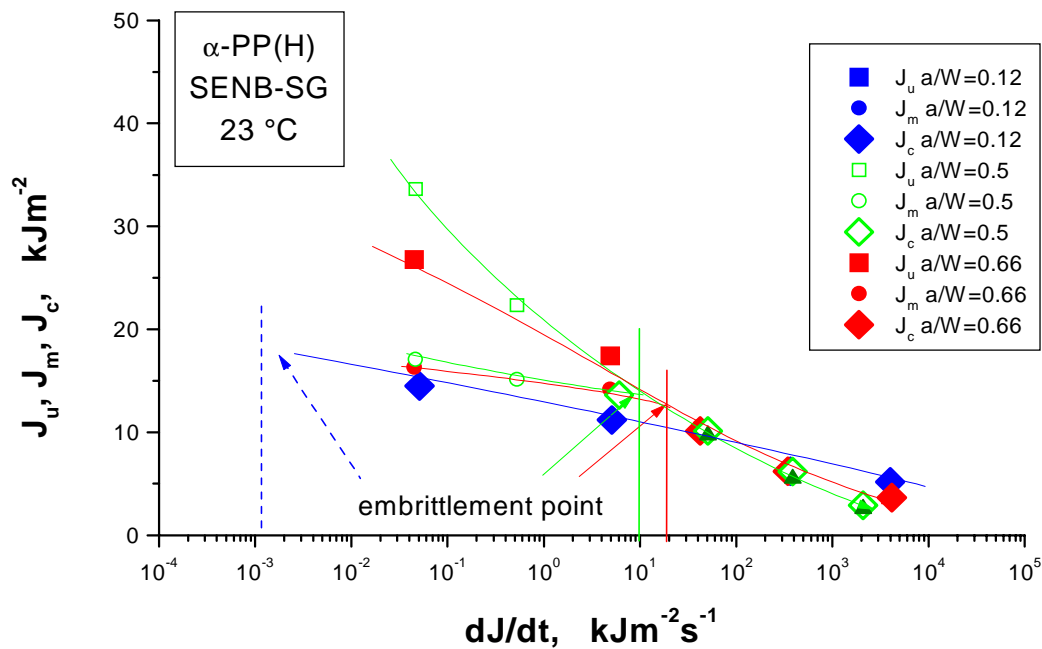


Fig. 8: Loading rate dependence of various J-integral values for the SENB-SG specimen configuration with different crack length (material: α -PP(H))

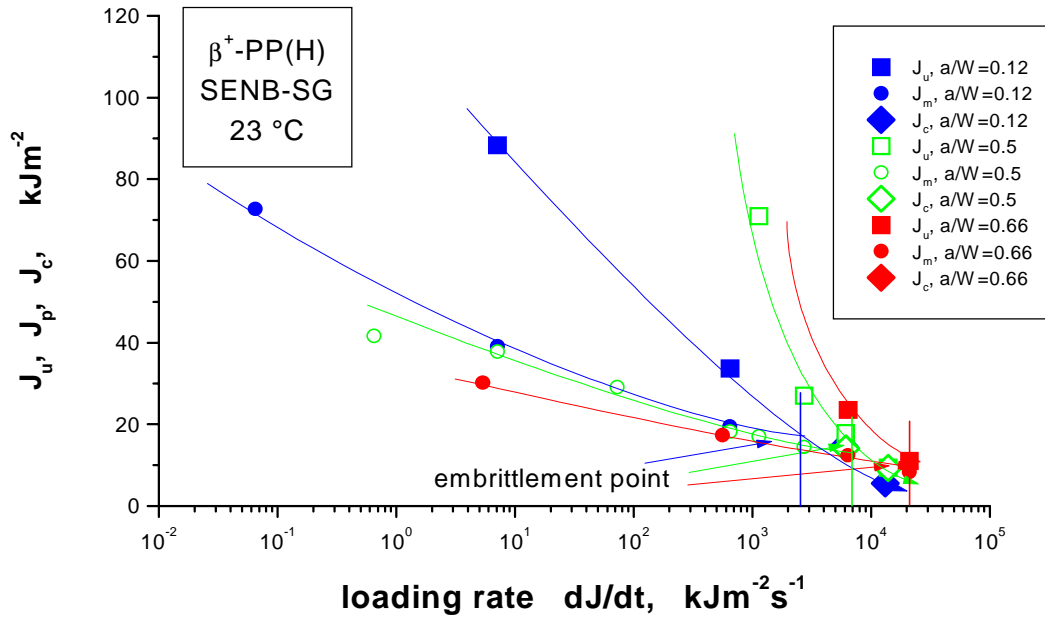


Fig. 9: Loading rate dependence of various J-integral values for the SENB-SG specimen configuration with different crack length (material: β^+ -PP(H))

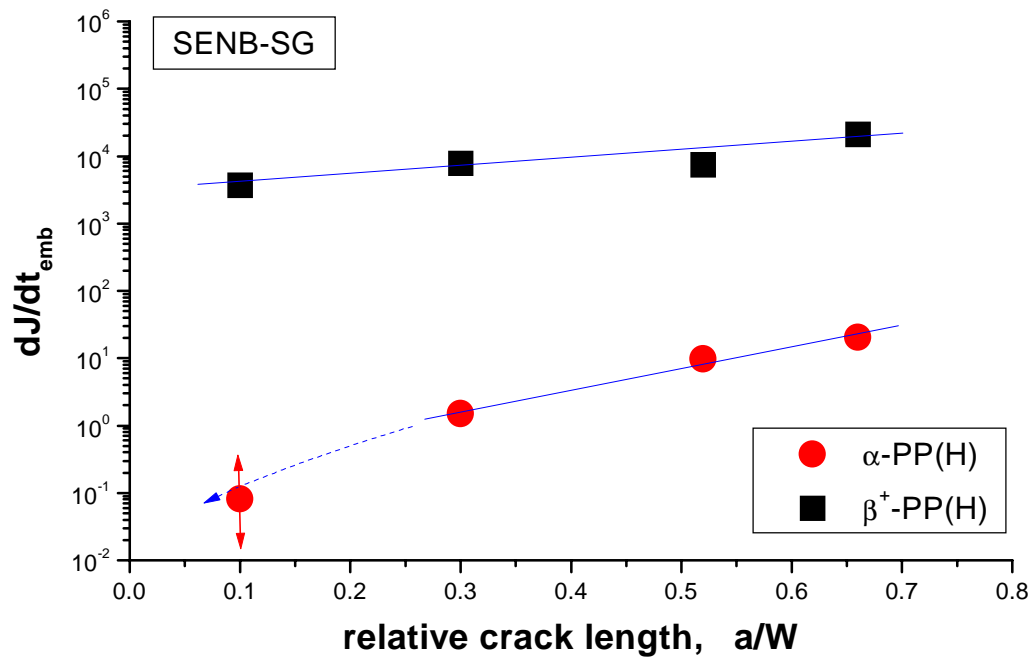


Fig. 10: Embrittlement points in terms of local loading rate, dJ/dt , as function of relative crack length for SENB-SG specimens